2012

Hybrid Rod-Like and Bent-Core Liquid Crystal Dimers Exhibiting Biaxial Smectic a and Nematic Phases

Yan Wang, *Kent State University - Kent Campus*
Hyung Guen Yoon, *Kent State University - Kent Campus*
Hari Krishna Bisoyi, *Kent State University - Kent Campus*
Satyendra Kumar, *Kent State University - Kent Campus*
Quan Li, *Kent State University - Kent Campus*

Journal of Materials Chemistry

Cite this: *J. Mater. Chem.*, 2012, **22**, 20363

www.rsc.org/materials

PAPER

Hybrid rod-like and bent-core liquid crystal dimers exhibiting biaxial smectic A and nematic phases

Yan Wang, Hyung Guen Yoon, Hari Krishna Bisoyi, Satyendra Kumar and Quan Li*

Received 4th July 2012, Accepted 9th August 2012
DOI: 10.1039/c2jm34315k

Liquid crystal hybrid dimers involving bent-core units and rod-like units were designed, synthesized and investigated by a combination of polarizing optical microscopy (POM), differential scanning calorimetry (DSC) and X-ray diffraction studies. All the four unsymmetrical dimers **1–4** exhibited stable nematic phases over a wide temperature range. Moreover, dimer **1** exhibited the biaxial smectic A (SmA) phase and dimer **2** exhibited a highly ordered mesophase below the nematic (N) phase. Two rod-like and bent-core nematogenic units were covalently linked in dimers **3** and **4** to furnish exclusively the nematic phase. The observation of the biaxial SmA phase underlying the nematic phase in one of the bent-core–rod dimers **1** would be a significant step forward towards achieving the biaxial nematic phase and resolving controversies related to the presence of cybotactic groups.

Introduction

Liquid crystals (LCs) are unique functional soft materials which simultaneously exhibit both order and mobility at molecular and macroscopic levels. The most successful commercial applications of LCs are in LC display (LCD) devices, where uniaxial rod-like nematic LCs are the active components while their uniaxial discotic nematic counterparts are employed in optical compensation films to widen the viewing angle and increase the contrast ratio of current LCDs.[1,2] The biaxial nematic phase has been rather elusive, nevertheless it has been envisaged that the use of a biaxial nematic phase could result in LCDs with faster refresh rates and dramatically lower power consumption thereby facilitating the next generation of LCDs with enhanced switching performance. Moreover, it is of great scientific significance in soft matter physics.[3–7] Theoretical studies have shown that mixtures of rods and discs could exhibit the biaxial nematic phase. However in practice, physical mixtures of rods and discs phase separate into two uniaxial nematic regions.[8] The need to overcome this difficulty has prompted the synthesis[9–11] of complex molecules consisting of covalently linked rod-like and discotic mesogenic units either terminally or laterally *via* flexible alkyl spacers. However it appears that these compounds fail to exhibit a stable biaxial nematic phase.

Bent-core (banana) LCs revitalized the field of LCs by exhibiting phases with polar order and phase chirality without the mesogens being chiral.[12–15] They were also investigated for the presence of the thermotropic biaxial nematic phase.[16–22] This is partly driven by the prediction that the nematic phase occurring in bent-core systems is more amenable to the formation of the biaxial nematic phase due to their intrinsic biaxial molecular shape.[3,4] However, the current trend in the search for the biaxial nematic phase is to covalently attach rod-like and bent-core mesogens *via* flexible spacers.[23–29] The study of the dependence of molecular shape on the resultant liquid crystalline phase of such amphiphilic and unsymmetric mesogenic dimers should also provide greater insight into their structure–property relationships and interesting new phase structures and phase sequences.[30–36] Moreover, these dimers represent compounds at the boundary between banana-shaped and rod-like LCs with combined exceptional properties and exhibit both banana phases and rod-like phases in the same compound. Interestingly, some of the dimers have been reported to exhibit a field induced biaxial nematic phase.[37] However, despite many promising properties, such non-symmetric twin molecules have not yet been extensively explored. In continuation of our effort towards the biaxial nematic phase,[38] here we report the synthesis and properties of four LC non-symmetric hybrid dimers **1–4** containing five-ring bent-core units terminally linked to an alkoxycyanobiphenyl rod-like unit *via* flexible spacers. Nematic phases, stable over a broad temperature range, have been observed for all the four compounds. Additionally, compound **1** exhibited the biaxial SmA phase as revealed by conoscopy observations while compound **2** showed a highly ordered mesophase below the nematic phase.

Results and discussion

The chemical structures of the newly designed and synthesized target compounds are shown in Scheme 1. All the compounds have been fully characterized by a combination of spectral techniques, elemental analysis, and mass spectrometry. As can be seen from the scheme, these bent-core–rod dimers contain

Liquid Crystal Institute, Kent State University, Kent, Ohio 44242, USA. E-mail: qli1@kent.edu; Fax: +1-330-672-2796; Tel: +1-330-672-1537

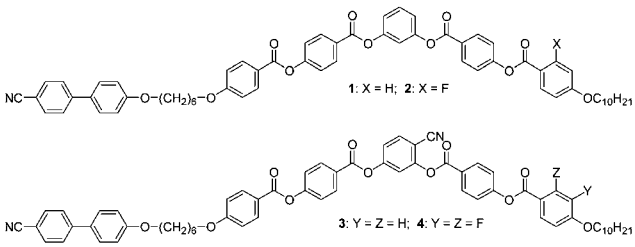

Scheme 1 Chemical structures of the synthesized unsymmetrical liquid crystal dimers.

alkoxycyanobiphenyl as the rod-like mesogenic unit and a five-ring bent-core derived either from resorcinol or 4-cyanoresorcinol bisbenzoates as the bent-core mesogenic unit. The mesomorphic properties of compounds **1–4** were studied by polarizing optical microscopy, differential scanning calorimetry, and synchrotron X-ray diffraction studies. The optical biaxiality of the liquid crystalline phases was investigated by conoscopy observations.

The phase behaviors and transition temperatures between various phases of the new dimers were initially observed under polarizing optical microscope (POM) and then confirmed by differential scanning calorimetry (DSC) experiments. Phase sequences and transition temperatures of all the compounds are summarized in Table 1.

Compound **1** exhibited a stable enantiotropic N phase at high temperatures and a monotropic smectic phase below the N phase on cooling from the isotropic phase. Under polarizing optical microscopy, the N phase exhibited a *Schlieren* texture whereas the lower temperature phase displayed a focal conic texture characteristic of the SmA phase as shown in Fig. 1. While cooling from the isotropic phase in homeotropically aligned cells, this compound exhibited a typical Schlieren texture in the N phase and focal conic texture in the smectic phase as shown in Fig. 1. Upon transition to the smectic phase, initially a focal conic texture appeared and then, on annealing for 30 s, it spontaneously changed to a marble texture in the homeotropically aligned cell but in a homogeneously aligned cell, the focal conic texture (Fig. 1f) was maintained. Upon slow cooling (<1 °C) from the isotropic phase, a uniform homeotropic alignment of compound **1** can be achieved for both the nematic and smectic phases in homeotropically aligned cells. The ability to obtain large homeotropic domains led us to investigate the possibility of phase biaxiality of the nematic and SmA phases *via* observing their optical biaxiality by conoscopy.

The homeotropically aligned N phase displayed a Maltese cross of isogyres as shown in Fig. 2a which suggests the uniaxial nature of the N phase. With homeotropic boundary conditions,

Table 1 Phase transition temperatures of the new mesogens obtained from DSC (peak temperature, °C) during heating and cooling cycles at a scan rate of 5 °C min^{-1}. Cr = crystalline, N = nematic phase, SmA_b = biaxial smectic A, I = isotropic phase

Dimer	Heating	Cooling
1	Cr 121.3 N 163.8 I	I 161.8 N 110.7 SmA_b 93.8 Cr
2	Cr 122.4 N 154.8 I	I 151.9 N 103.2 SmX 83.6 Cr
3	Cr 90.0 N 183.3 I	I 181.9 N < 60 glassy
4	Cr 115.0 N 181.0 I	I 179.6 N < 55 glassy

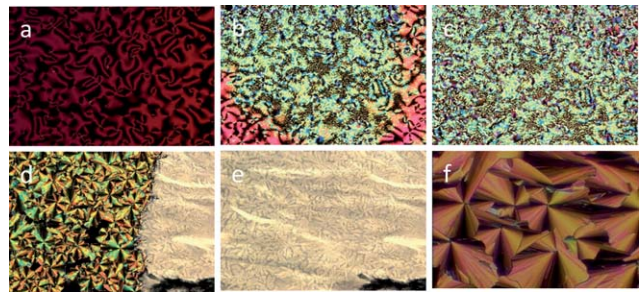

Fig. 1 POM textures of compound **1** in the nematic phase at (a) 161 °C, (b) 142 °C and (c) 140 °C. Textures in the smectic phase were recorded at (d) 110 °C, (e) 110 °C after annealing for 30 s in a homeotropically aligned cell, and (f) 105 °C in a homogenously aligned cell.

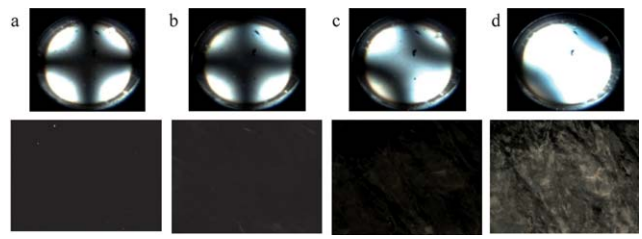

Fig. 2 Photomicrographs of the conoscopic patterns (top) and the corresponding polarizing microscopy textures of homeotropically aligned cells (bottom) of compound **1** in: (a) the uniaxial N phase at 123 °C, and (b–d) the biaxial SmA phase at 108 °C. Between crossed polarizers, the sample was rotated by (b) 0°, (c) clockwise by 10° and (d) clockwise by 20°. Separation of the isogyres confirms the optical biaxiality of the SmA phase. The optical biaxiality was very high as judged from the isogyres remaining out of the field of view for sample rotation between 20° and 65°.

this cross in the SmA phase changes into two arch-shaped isogyres that are separated by a distance that increases as the sample is rotated between crossed polarizers. This result confirms that the SmA phase is optically biaxial.[39–41] This observation of the biaxial SmA phase below the N phase in compound **1** is very promising. It provides a pathway towards understanding the formation of the much sought after biaxial nematic phase in thermotropic LCs through investigations of homologs of compound **1** and compounds having a closely related structure.

Compound **2**, which contains an additional fluoro-substitution in one of the wings of the bent-core unit, exhibited a phase behavior similar to **1**. Its melting temperature is comparable to that of compound **1**, however, both isotropic and crystallization temperatures are lower. The monotropic mesophase which appears below the N phase exhibited by compound **2** seems to be a highly ordered mesophase. A homeotropic cell of this compound observed under polarizing optical microscope displayed a Schlieren texture in the N phase while the lower temperature mesophase displayed a fan-shaped texture as shown in Fig. 3.

The fan-shaped texture indicates that this could be a highly ordered lamellar or columnar phase. The N phase of compound **2** was found to be uniaxial in nature based on the observation of a dark homeotropic state displaying the Maltese cross (Fig. 3c). However, the lower temperature phase failed to exhibit a homeotropic alignment.

In order to enhance the tendency to form the N phase of the dimeric mesogens, a 4-cyanoresorcinol bisbenzoate core was

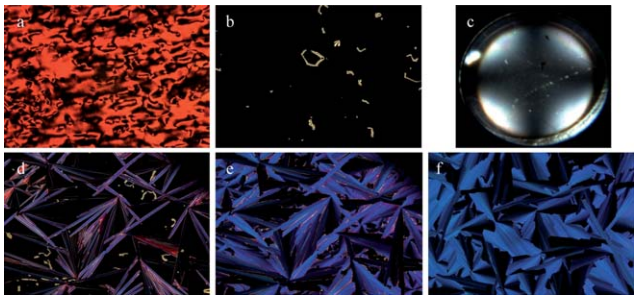

Fig. 3 POM textures of compound **2** in a homeotropically aligned cell in the nematic phase (a) at 140 °C and (b) at 130 °C; conoscopy pattern (c) in the homeotropic state at 110 °C and textures of the lower temperature lamellar phase (d) at 104 °C, (e) at 103 °C, and (f) at 100 °C.

introduced as the bent-core mesogenic unit. This unit is known to favor the formation of stable N phases.[42–44] As anticipated, compound **3** exhibited exclusively N mesomorphism over a wide temperature range. Upon heating, it melted into the N phase before reaching the isotropic state. Upon cooling the isotropic state, the N phase appeared and the compound solidified below 60 °C without apparent crystallization, as observed under the microscope. Compound **4** was synthesized by introducing difluoro-substitution onto one of the wings of the bent-core unit. In a manner similar to **3**, this compound also exhibited exclusively the N phase. It is interesting to note that the monotropic higher order phases observed in both compounds **1** and **2** are completely suppressed in compounds **3** and **4**. Moreover, the N phase was better stabilized in **3** and **4** because of their lower melting points and higher isotropic transition temperatures as compared to **1** and **2**. Compounds **3** and **4** did not seem to crystallize but instead vitrified in the N phase, *i.e.*, passed to a glassy state upon cooling from the isotropic state. During subsequent heating and cooling cycles, only the N to isotropic transitions were observed in both compounds **3** and **4**. Typical Schlieren textures were noticed for compound **3** in homeotropically aligned cells as shown in Fig. 4.

In homeotropic cells, large single homeotropic domain formation of compound **4** was seen while cooling from the isotropic phase, as shown in Fig. 5. Conoscopy studies of the homeotropic state of compound **4** did not indicate any optical biaxiality in its N phase since it displayed the cross of isogyres as shown in Fig. 5d.

The structures of liquid crystalline phases of the dimers were investigated by synchrotron X-ray diffraction studies. The occurrence of nematic phases over a broad temperature range allowed us to study the nematic phase at different temperatures. Fig. 6 shows the X-ray diffraction patterns of compound **1** in the N phase.

This compound was well oriented in the N phase and two sets of diffuse reflections are observed in the diffraction pattern. The small angle diffraction peak corresponds to an average molecular

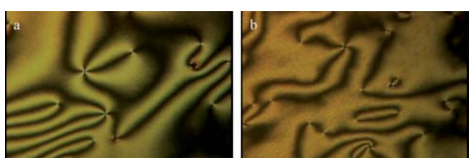

Fig. 4 POM textures of compound **3** in a homeotropic aligned cell (a) at 179 °C and (b) at 176 °C.

Fig. 5 POM textures of compound **4** in the homeotropic aligned cell (a) at 178 °C, (b) at 175 °C, and (c) at 65 °C. (d) Conoscopic pattern of compound **4** in the nematic phase in homeotropic dark state at 173 °C.

length of 58.7 Å while the wide-angle diffraction peak corresponds to a lateral separation of 4.5 Å of the molecules in the N phase. The overall X-ray diffraction pattern did not change much at lower temperature except for an increase in the intensity of the small angle peak, indicating better organization of the molecules and enhancement of the orientational order parameter at lower temperatures. The X-ray diffraction pattern at temperature below the N phase of **1** displayed multiple sharp reflections in the small angle region. The *d*-spacing 56 Å in the smectic phase is comparable to the molecular length (~61 Å), and this phase was identified as the smectic A phase, consistent with the textural observations.

The X-ray diffraction pattern of compound **2** in the N phase is similar to that of compound **1** as shown in Fig. 7. Both the wide angle and small angle reflections were diffused, which is typical of the N phases. In the lower temperature phase, compound **2** exhibited several sharp rings, as shown in Fig. 7b. The *d*-value (83.5 Å) calculated from the lowest angle reflection corresponds to a value which is larger than the molecular length but less than twice the molecular length. This indicates that the lower temperature mesophase could be a highly ordered smectic phase with partial interdigitation of molecules. However, the nature of the exact phase structure needs further detailed investigation.

Since both compounds **3** and **4** exhibit similar phase behaviors, an X-ray study of compound **4** was undertaken and the results are shown in Fig. 8. The X-ray diffraction patterns of compound **4** are typical of the N phase having two diffuse reflections, one in the small angle region while the other in the wide angle region. As expected, lowering the temperature in the N phase seems to promote better organization of the molecules with reduced molecular mobility which is reflected in the relatively narrow and intense diffraction peaks as shown in Fig. 8.

Experimental section

Instrumentation

All starting materials, solvents and reagents were purchased from Sigma-Aldrich company and used without further purification.

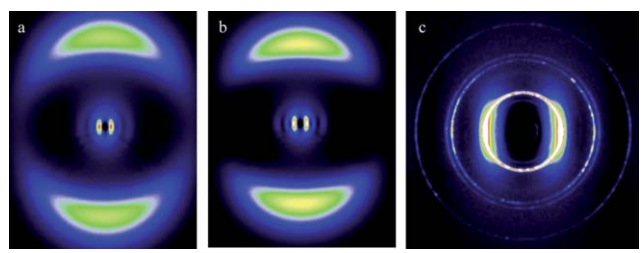

Fig. 6 X-ray diffraction patterns of the aligned sample of compound **1** in the N phase (a) at 149 °C and (b) at 112 °C, and in the SmA phase (c) at 108 °C.

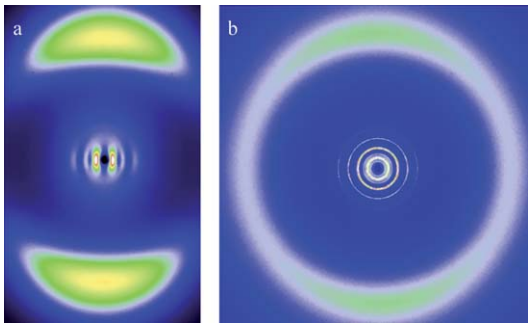

Fig. 7 X-ray diffraction patterns of compound **2** in the nematic phase (a) at 121.4 °C and in the highly ordered unidentified lamellar phase (b) at 107 °C.

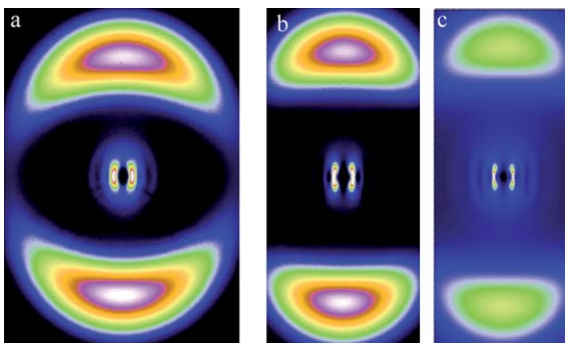

Fig. 8 X-ray diffraction patterns of the aligned sample of compound **4** in the nematic phase (a) at 176 °C, (b) at 131 °C, and (c) at 94 °C.

Column chromatography was carried out on silica gel (230–400 mesh). Analytical thin layer chromatography (TLC) was performed on commercially coated 60 mesh F254 glass plates. ^{1}H and ^{13}C NMR spectra were recorded on a Varian Gemini 200 or on a Bruker 400 spectrometer. Chemical shifts are reported in units (ppm) with the residual solvent peak as internal standard. Calorimetric measurements were performed on a Perkin-Elmer differential scanning calorimeter (scanning rate 5 °C min^{-1}). Transition temperatures were taken at the maximum of transition peaks. Mass spectra were taken at the Mass Spectrometry & Proteomics Facility of Ohio State University. Elemental analysis was performed by Robertson Microlet Inc. Texture changes were observed by optical microscopy using a Leitz polarizing microscope with a temperature controller or a Nikon polarizing microscope. Synchrotron X-ray diffraction studies were carried out at the advanced photon source of Argonne national laboratory. Samples were filled in a 2 mm quartz capillary and aligned by cooling from the isotropic phase in the presence of a magnetic field of approximately 2.5 kG, applied perpendicular to the X-ray beam. XRD patterns were acquired using an MAR-3450 area detector placed at a distance of 497.9 mm from the sample and an X-ray wavelength of 0.765335 Å was selected.

Analytical data of compound 1. ^{1}H NMR (400 MHz, $CDCl_3$) δ 8.29–8.27 (m, 4H, ArH), 8.17–8.14 (m, 4H, ArH), 7.71–7.68 (m, 2H, ArH), 7.65–7.61 (m, 2H, ArH), 7.54–7.43 (m, 3H, ArH), 7.38 (d, 2H, J = 8.8 Hz, ArH), 7.37 (d, 2H, J = 8.8 Hz, ArH), 7.22–7.18 (m, 3H, ArH), 7.02–6.98 (m, 6H, ArH), 4.13–4.02 (m, 6H, –OCH_2–), 1.93–1.28 (m, 24H, –CH_2–), 0.89 (t, 3H, J = 6.8 Hz, –CH_3); ^{13}C NMR (100 MHz, $CDCl_3$) δ 164.3, 164.2, 164.1, 164.0, 183.8, 163.7, 159.7, 155.4, 155.4, 151.4, 145.2, 132.6, 132.5 (×2), 132.4 (×2), 132.4 (×2), 131.8 (×2), 129.9, 128.9, 128.3 (×2), 127.1, 127.0 (×2), 126.6, 126.6, 126.4, 122.1 (×2), 122.1 (×2), 121.0, 120.9, 119.3, 119.1, 115.8, 115.0 (×2), 114.4 (×2), 114.4 (×2), 113.4, 110.0, 68.4, 68.1, 67.9, 31.9, 29.5, 29.3, 29.3, 29.1, 29.0, 29.0, 26.0, 25.8, 25.8, 25.7, 22.7, 14.1; HRMS m/z calcd for $C_{63}H_{61}NO_{11}Na^+$ (M + Na^+): 1030.4142, found: 1030.4113; elemental analysis calcd for $C_{63}H_{61}NO_{11}$: C 75.06, H 6.10, N 1.39, found: C 74.78, H 5.94, N 1.38%.

Analytical data of compound 2. ^{1}H NMR (400 MHz, $CDCl_3$) δ 8.29–8.27 (m, 4H, ArH), 8.17–8.15 (m, 2H, ArH), 8.06 (dd, 1H, J = 8.8, 8.4 Hz, ArH), 7.72–7.70 (m, 2H, ArH), 7.65–7.61 (m, 2H, ArH), 7.55–7.43 (m, 3H, ArH), 7.40–7.36 (m, 4H, ArH), 7.21–7.18 (m, 3H, ArH), 7.01–6.98 (m, 4H, ArH), 6.79 (dd, 1H, J = 9.2, 2.8 Hz, ArH), 6.70 (dd, 1H, J = 12.8, 2.0 Hz, ArH), 4.13–4.02 (m, 6H, –OCH_2–), 1.90–1.28 (m, 24H, –CH_2–), 0.89 (t, 3H, J = 6.8 Hz, –CH_3); ^{13}C NMR (50 MHz, $CDCl_3$) δ 166.7, 165.2, 165.0, 164.2, 164.0, 163.7, 161.9, 161.8, 161.5, 159.7, 155.4, 155.1, 151.4 (×2), 145.2, 133.9, 132.6, 132.5 (×2), 132.4 (×2), 131.8 (×2), 131.4, 129.9, 128.3 (×2), 127.0 (×2), 126.7, 126.6, 122.1 (×2), 121.0, 119.3, 119.1, 115.8, 115.0 (×2), 114.4 (×2), 111.0, 110.1, 109.4, 109.2, 103.2, 102.6, 68.9, 68.1, 67.9, 31.9, 29.5 (×3), 29.3 (×3), 29.1, 29.0, 28.9, 25.9, 22.6, 14.1. MS m/z calcd for $C_{63}H_{61}NO_{11}Na^+$ (M + Na^+): 1048, found: 1048; elemental analysis calcd for $C_{63}H_{61}NO_{11}$: C 73.74, H 5.89, N 1.36, found: C 73.48, H 5.74, N 1.32%.

Analytical data of compound 3. ^{1}H NMR (400 MHz, $CDCl_3$) δ 8.34–8.32 (m, 2H, ArH), 8.28–8.26 (m, 2H, ArH), 8.16 (dd, 4H, J = 9.2, 2.0 Hz, ArH), 7.80 (d, 1H, J = 8.8 Hz, ArH), 7.72–7.68 (m, 2H, ArH), 7.65–7.61 (m, 2H, ArH), 7.54–7.52 (m, 2H, ArH), 7.46–7.38 (m, 5H, ArH), 7.33 (dd, 1H, J = 8.8, 2.0 Hz, ArH), 7.02–7.98 (m, 6H, ArH), 4.13–4.03 (m, 6H, –OCH_2–), 1.93–1.28 (m, 24H, –CH_2–), 0.89 (t, 3H, J = 6.8 Hz, –CH_3); ^{13}C NMR (50 MHz, $CDCl_3$) δ 164.2, 163.8, 163.8, 163.2, 162.9, 159.7, 156.0, 155.8, 155.0, 154.8, 153.4, 145.2, 143.9, 133.9, 132.6 (×2), 132.5 (×2), 132.4 (×3), 132.2 (×2), 132.0 (×2), 128.9, 128.3, 127.1, 127.0, 126.4, 125.7, 125.3, 123.7, 122.4 (×2), 122.3 (×2), 120.9, 120.8, 120.0, 117.4, 115.0, 114.8, 114.4 (×3), 113.5, 104.2, 69.1, 68.4, 68.1, 31.8, 29.5 (×2), 29.3 (×2), 29.3 (×2), 29.0, 29.0, 25.9, 25.7, 22.6, 14.1. MS m/z calcd for $C_{63}H_{61}NO_{11}Na^+$ (M + Na^+): 1055, found: 1055; elemental analysis calcd for $C_{63}H_{61}NO_{11}$: C 74.40, H 5.85, N 2.71, found: C 74.13, H 5.68, N 2.69%.

Analytical data of compound 4. ^{1}H NMR (400 MHz, $CDCl_3$) δ 8.34 (d, 2H, J = 9.2 Hz, ArH), 8.27 (d, 2H, J = 8.8 Hz, ArH), 8.15 (dd, 2H, J = 9.2, 1.2 Hz, ArH), 7.89–7.84 (m, 1H, ArH), 7.80 (d, 1H, J = 8.0 Hz, ArH), 7.71–7.68 (m, 2H, ArH), 7.65–7.61 (m, 2H, ArH), 7.55–7.52 (m, 2H, ArH), 7.46–7.38 (m, 5H, ArH), 7.33 (dd, 1H, J = 8.8, 2.4 Hz, ArH), 7.02–6.98 (m, 4H, ArH), 6.86–6.82 (m, 1H, ArH), 4.16–4.02 (m, 6H, –OCH_2–), 1.95–1.28 (m, 24H, –CH_2–), 0.89 (t, 3H, J = 6.8 Hz, –CH_3); ^{13}C NMR (50 MHz, $CDCl_3$) δ 164.2, 163.8, 163.2, 162.8, 159.7, 155.8, 155.4, 155.0, 154.8, 153.4, 145.2, 143.9, 133.9, 132.6 (×2), 132.5 (×2), 132.4 (×2), 132.2 (×2), 132.0 (×2), 128.9, 128.3 (×2), 127.1 (×2), 127.0, 126.4, 125.7, 125.6, 122.3 (×2), 122.2 (×2), 120.8, 120.0,

117.4, 115.0 (×2), 114.7, 114.4 (×2), 113.5, 110.7, 108.5, 104.2, 70.0, 69.0, 68.1, 31.8 (×2), 29.5 (×2), 29.2 (×2), 29.1, 28.9 (×2), 25.7 (×2), 22.6, 14.1. MS *m/z* calcd for $C_{63}H_{61}NO_{11}Na^+$ (M + Na^+): 1091, found: 1091; elemental analysis calcd for $C_{63}H_{61}NO_{11}$: C 71.90, H 5.47, N 2.62, found: C 71.59, H 5.26, N 2.66%.

Conclusions

We have designed and synthesized four new mesogens incorporating non-symmetric dimers with one bent-core and another rod-like mesogenic unit and studied their LC properties. Compounds **3** and **4** exhibited exclusively the nematic phase over a broad temperature range. Compounds **1** and **2** also exhibited N phases and higher order phases at lower temperatures. The low temperature lamellar phase of compound **1** was found to be the biaxial SmA phase. It has been predicted that if the lower temperature SmA phase is biaxial, then the high temperature nematic phase may also be biaxial.[45] However, we observed only a uniaxial N to biaxial SmA phase transition. The observation of the biaxial SmA phase in this system is of special interest in the light of the expectation of fast switching processes for this phase.[46–48] Such fast switching rates would be needed for improving and expanding the utility of LC displays. Moreover, to fabricate a display device, it is usually required to first properly align a nematic phase and then it is cooled to obtain a defect-free smectic structure. For this reason the observation of biaxial SmA and the N phases in a single compound is an important advancement towards their application in new LCD technologies. The occurrence of the N phase above the biaxial SmA phase in compound **1** is expected to provide a pathway to the formation of the biaxial N phase in these shape amphiphiles.

Acknowledgements

The work is supported by the US Department of Energy (DOE DE-SC0001412). Use of the Advanced Photon Source (APS) was supported by the Department of Energy, Basic Energy Sciences (BES), Office of Science, under contract no. W-31-109-Eng-38. The Midwestern Universities Collaborative Access Team's (MUCAT) sector at the APS is supported by the U.S. DOE, BES, Office of Science, through the Ames Laboratory under contract no. W-7405-Eng-82.

References

1 H. Mori, *J. Disp. Technol.*, 2005, **1**, 179–186.
2 K. Kawata, *Chem. Rec.*, 2002, **2**, 59–80.
3 G. R. Luckhurst, *Thin Solid Films*, 2001, **393**, 40–52.
4 G. R. Luckhurst, *Angew. Chem., Int. Ed.*, 2005, **44**, 2834–2836.
5 D. W. Bruce, *Chem. Rec.*, 2004, **4**, 10–22.
6 C. Tschierske and D. J. Photinos, *J. Mater. Chem.*, 2010, **20**, 4263–4294.
7 M. Lehmann, *Liq. Cryst.*, 2011, **38**, 1389–1405.
8 M. J. Freiser, *Phys. Rev. Lett.*, 1970, **24**, 1041–1043.
9 I. D. Fletcher and G. R. Luckhurst, *Liq. Cryst.*, 1995, **18**, 175–183.
10 R. W. Date and D. W. Bruce, *J. Am. Chem. Soc.*, 2003, **125**, 9012–9013.
11 P. H. J. Kouwer and G. H. Mehl, *J. Am. Chem. Soc.*, 2003, **125**, 11172–11173.
12 G. Pelzl, S. Diele and W. Weissflog, *Adv. Mater.*, 1999, **11**, 707–724.
13 R. A. Reddy and C. Tschierske, *J. Mater. Chem.*, 2006, **16**, 907–961.
14 H. Takezoe and Y. Takanishi, *Jpn. J. Appl. Phys.*, 2006, **45**, 597–625.
15 J. Etxebarria and M. B. Ros, *J. Mater. Chem.*, 2008, **18**, 2919–2926.
16 B. R. Acharya, S. Primak and S. Kumar, *Phys. Rev. Lett.*, 2004, **92**, 145506.
17 L. A. Madsen, T. J. Dingemans, M. Nakata and E. T. Samulski, *Phys. Rev. Lett.*, 2004, **92**, 145505.
18 V. Prasad, S. W. Kang, K. A. Suresh, L. Joshi, Q. Wang and S. Kumar, *J. Am. Chem. Soc.*, 2005, **127**, 17224–17227.
19 Y. Jang, V. P. Panov, A. Kocot, J. K. Vij, A. Lehmann and C. Tschierske, *Appl. Phys. Lett.*, 2009, **95**, 183304.
20 K. V. Le, M. Mathews, M. Chambers, J. Harden, Q. Li, H. Takezoe and A. Jakli, *Phys. Rev. E: Stat., Nonlinear, Soft Matter Phys.*, 2009, **79**, 030701.
21 H.-G. Yoon, S.-W. Kang, R. Y. Dong, A. Marini, K. A. Suresh, M. Srinivasarao and S. Kumar, *Phys. Rev. E: Stat., Nonlinear, Soft Matter Phys.*, 2010, **81**, 051706.
22 M. S. Park, B.-J. Yoon, J. O. Park, V. Prasad and M. Srinivasarao, *Phys. Rev. Lett.*, 2010, **105**, 027801.
23 C. V. Yelamaggad, S. K. Prasad, G. G. Nair, I. S. Shashikala, D. S. S. Rao, C. V. Lobo and S. Chandrasekhar, *Angew. Chem., Int. Ed.*, 2004, **43**, 3429–3432.
24 M. G. Tamba, B. Kosata, K. Pelz, S. Diele, G. Pilzl, Z. Vakhovskaya, H. Kresse and W. Weissflog, *Soft Matter*, 2006, **2**, 60–65.
25 M. G. Tamba, U. Baumeister, G. Pelzl and W. Weissflog, *Liq. Cryst.*, 2010, **37**, 853–874.
26 M. G. Tamba, A. Bobrovsky, V. Shibaev, G. Pelzl, U. Baumeister and W. Weissflog, *Liq. Cryst.*, 2011, **38**, 1531–1550.
27 G. Lee, H.-C. Jeong, F. Araoka, K. Ishikawa, J. G. Lee, K.-T. Kang, M. Cepic and H. Takezoe, *Liq. Cryst.*, 2010, **37**, 883–892.
28 C. V. Yelamaggad, I. S. Shashikala, G. Liao, D. S. S. Rao, S. K. Prasad, Q. Li and A. Jakli, *Chem. Mater.*, 2006, **18**, 6100–6102.
29 G. Shanker, M. Prehm and C. Tschierske, *J. Mater. Chem.*, 2012, **22**, 168–174.
30 P. Kumar, U. S. Hiremath, C. V. Yelamaggad, A. G. Rossberg and K. S. Krishnamurthy, *J. Phys. Chem. B*, 2008, **112**, 9270–9274.
31 P. Kumar, U. S. Hiremath, C. V. Yelamaggad, A. G. Rossberg and K. S. Krishnamurthy, *J. Phys. Chem. B*, 2008, **112**, 9753–9760.
32 P. Kumar, Y. G. Marinov, H. P. Hinov, U. S. Hiremath, C. V. Yelamaaggad, K. S. Krishnamurthy and A. G. Petrov, *J. Phys. Chem. B*, 2009, **113**, 9168–9174.
33 G. Liao, I. Shashikala, C. V. Yelamaggad, D. S. S. Rao, S. K. Prasad and A. Jakli, *Phys. Rev. E: Stat., Nonlinear, Soft Matter Phys.*, 2006, **73**, 051701.
34 A. Jakli, G. Liao, I. Shashikala, U. S. Hiremath and C. V. Yelamaggad, *Phys. Rev. E: Stat., Nonlinear, Soft Matter Phys.*, 2006, **74**, 041706.
35 J. Heuer, R. Stannarius, M.-G. Tamba and W. Weissflog, *Phys. Rev. E: Stat., Nonlinear, Soft Matter Phys.*, 2008, **77**, 056206.
36 M. -G. Tamba, W. Weissflog, A. Eremin, J. Heuer and R. Stannarius, *Eur. Phys. J. E*, 2007, **22**, 85–95.
37 R. Stannarius, A. Eremin, M.-G. Tamba, G. Pelzl and W. Weissflog, *Phys. Rev. E: Stat., Nonlinear, Soft Matter Phys.*, 2007, **76**, 061704.
38 M. Mathews, S. Kang, S. Kumar and Q. Li, *Liq. Cryst.*, 2011, **38**, 31–40.
39 B. K. Sadashiva, R. A. Reddy, R. Pratibha and N. V. Madhusudana, *J. Mater. Chem.*, 2002, **12**, 943–950.
40 R. A. Reddy and B. K. Sadashiva, *J. Mater. Chem.*, 2004, **14**, 310–319.
41 L. Pan, B. K. McCoy, S. Wang, W. Weissflog and C. C. Huang, *Phys. Rev. Lett.*, 2010, **105**, 117802.
42 L. Kovalenko, M. W. Schroder, R. A. Reddy, S. Diele, G. Pelzl and W. Weissflog, *Liq. Cryst.*, 2005, **32**, 857–865.
43 C. Keith, A. Lehmann, U. Baumeister, M. Prehm and C. Tschierske, *Soft Matter*, 2010, **6**, 1704–1721.
44 G. Shanker, M. Prehm, M. Nagaraj, J. K. Vij and C. Tschierske, *J. Mater. Chem.*, 2011, **21**, 18711–18714.
45 H. R. Brand and H. Pleiner, *Makromol. Chem. Rapid Commun.*, 1991, **12**, 539–545.
46 M. Nagaraj, Y. P. Panarin, J. K. Vij, C. Keith and C. Tschierske, *Appl. Phys. Lett.*, 2010, **97**, 213505.
47 Y. Shombo, Y. Takanishi, K. Ishikawa, E. Gorecka, D. Pociecha, J. Mieczkowski, K. Gomola and H. Takezoe, *Jpn. J. Appl. Phys.*, 2006, **45**, L282–L284.
48 R. A. Reddy, C. Zhu, R. Shao, E. Korblova, T. Gong, Y. Shen, E. Garcia, M. A. Glaser, J. E. Maclennan, D. M. Walba and N. A. Clark, *Science*, 2011, **332**, 72–77.